THE JOURNAL OF PHYSICAL CHEMISTRY B

pubs.acs.org/JPCB Article

Impact of PDMS-Based Microfluidics on Belousov–Zhabotinsky Chemical Oscillators

James Sheehy, Ian Hunter, Maria Eleni Moustaka, S. Ali Aghvami, Youssef Fahmy, and Seth Fraden*

Cite This: https://dx.doi.org/10.1021/acs.jpcb.0c08422 Read Online

ACCESS | Metrics & More | Article Recommendations | Supporting Information

ABSTRACT: Sub-nanoliter volumes of the Belousov–Zhabotinsky (BZ) reaction are sealed in microfluidic devices made from polydimethylsiloxane (PDMS). Bromine, which is a BZ reaction intermediate that participates in the inhibitory pathway of the reaction, is known to permeate into PDMS, and it has been suggested that PDMS and bromine can react (*J. Phys. Chem. A. 108*, **2004**, 1325–1332). We characterize the extent to which PDMS affects BZ oscillations by varying the volume of the PDMS surrounding the BZ reactors. We measure how the oscillation period varies with PDMS volume and compare with a theoretical reaction–diffusion model, concluding that bromine reacts with PDMS. We demonstrate that minimizing the amount of PDMS by making the samples as thin as possible maximizes the number of oscillations before the BZ reaction reaches equilibrium and ceases to oscillate. We also demonstrate that the deleterious effects of the PDMS–BZ interactions are somewhat mitigated by imposing constant chemical boundary conditions through using a light-sensitive catalyst, ruthenium, in combination with patterned illumination. Furthermore, we show that light can modulate the frequency and phase of the BZ oscillators contained in a PDMS matrix by 20–30%.

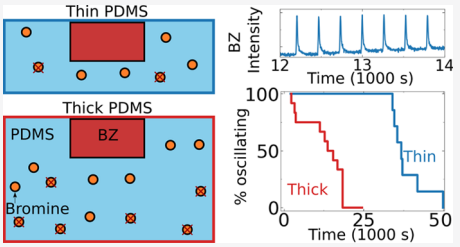

INTRODUCTION

Compartmentalization of the oscillatory Belousov–Zhabotinsky (BZ) chemical reaction as aqueous drops in a continuous oil phase serves as a means to create networks in which either inhibitory or excitatory BZ species permeate from one BZ compartment to another.[1−16] In an alternative approach, we demonstrated the engineering of reaction–diffusion networks employing the BZ reaction that were capable of producing a wide variety of spatiotemporal patterns, including that of central pattern generators found in living organisms. To build these networks, we employed methods from soft lithography to fabricate diffusively coupled networks using the elastomer polydimethylsiloxane (PDMS).[12,17] This method offers numerous advantages over the use of drops to create networks, and we demonstrated control of (i) the topology of the network, the (ii) boundary and (iii) initial conditions, (iv) the volume of each reactor, (v) the coupling strength, and (vi) whether the coupling was of an inhibitory or excitatory nature.[17] However, one limitation was that the thickness of the PDMS underneath each reactor had to be less than a few tens of microns thick for the networks to reliably support oscillations.

PDMS, an elastomer with a low dielectric constant, is expected to be permeable to those BZ chemicals that also have a low dielectric constant, e.g., nonpolar molecules, while PDMS is relatively impermeable to polar and charged species, such as water and acids.[18] In the most simplified description, each BZ reactant can be considered to belong to either the excitatory or inhibitory pathway. Ginn et al. studied the behavior of BZ in patterned PDMS microfluidic chips and hypothesized that bromine, an intermediary species associated with the inhibition of the BZ oscillations, permeates into and could possibly react with PDMS.[19] The chemical bromine reacts with malonic acid present in the BZ solution and generates bromide, which directly inhibits BZ oscillations. Bromide is charged and does not permeate through the PDMS. However, bromine readily diffuses through the PDMS, and if there are two compartments of BZ that are separated by PDMS, then bromine can pass between the compartments and act as a communicator of inhibition. The permeation and reaction properties of bromine in PDMS have been used to localize the site of bromine removal to disinhibit the BZ reaction, thereby initiating BZ waves by placing a block of PDMS in the BZ solution.[20] However, bromine is not the only BZ reactant that interacts with PDMS, as the bromine dioxide radical, which is part of the excitatory pathway, is also expected to partition into low dielectric constant materials.[21]

PDMS has been demonstrated to be a material that offers promise for creating functional networks of oscillating chemicals.[12,17] However, the fact that BZ chemicals permeate into and perhaps react with PDMS means that PDMS is not merely acting as a passive container of the BZ chemicals but is

Received: September 15, 2020
Revised: November 28, 2020

itself an active ingredient influencing the behavior of the oscillating chemical reaction.[22,23] Here, we study the simplest possible network, a single BZ oscillator sealed in a PDMS container, and investigate how oscillations are affected by the amount of PDMS surrounding the BZ solution.

In prior work, we established the use of the light-sensitive catalyst, ruthenium, to create regions of space of constant chemical conditions, which were used to isolate one chemical oscillator from another.[1,11,12,17,24] Here, we compare the behaviors of BZ oscillators in PDMS with and without light-controlled boundaries. In other previous works, we used light to control the frequency and phase of oscillators consisting of emulsions of BZ in oil.[24] Here, we characterize the extent to which the frequency and phase of BZ oscillators in PDMS can be controlled using light.

METHODS

To study the behavior of a single oscillator of BZ, we use soft-lithography manufacturing methods to precisely create the desired network topology and geometry in PDMS.[17,25] We refer to the compartment containing the BZ solution as a well. The typical width of the wells ($w \sim 100\ \mu$m) is small compared with the length scale of diffusion of bromine in water ($D \sim 10^{-5}$ cm^2 s^{-1}) over the duration of a BZ oscillation ($\tau \sim$300s), e.g., $w < \sqrt{D\tau}$, so the contents of each well remain well mixed (Figure 1). A square shape was chosen for this study as we plan

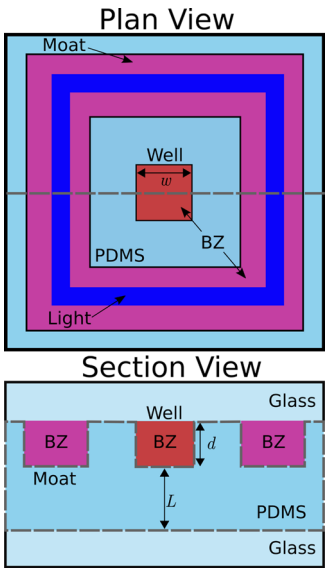

Figure 1. Plan and section view of a single well enclosed by a moat. The dotted gray line in the plan view denotes the location of the section view, where the dotted line denotes the PDMS profile. Initially, both moat and well contain the same BZ solution. Each well has width w and depth d and forms an isolated chamber filled with BZ (red), surrounded by PDMS (blue). Each well sits on top of a layer of PDMS of thickness L. The PDMS and BZ are sealed between two layers of glass (light blue). Blue light (dark blue) is projected onto the moat (purple) to set the BZ at a constant chemical condition.

to study pairs of wells in the near future, and the planar geometry simplifies modeling of the coupling between pairs of BZ oscillators.

The wells are isolated from each other by surrounding each well with a volume of BZ solution that is at steady state. We refer to this rectangular zone of nonoscillating BZ solution as a moat, evoking the isolation provided by the like-named water-filled ditch surrounding a castle, shown in Figure 1. The notations "well" and "moat" are consistent with terminology from our previous work.[17] The BZ in the moat is induced to remain at a fixed chemical state by using the photosensitive catalyst, $Ru(bpy)_3^{2+}$, which stops the BZ oscillations when exposed to sufficient light.[26] We apply the light to the moat with a 2 s period, with the light applied to the moat for 1 s and the light shut off for 1 s. Above a critical intensity, the applied light pushes the oscillating BZ off its limit cycle, suspending the BZ in a steady state with concentrations approximately equal to those of the reduced state in which the bromine concentration is low.

The similarities between the diffusion equation and Poisson's equation of electrostatics mean that the moat in this reaction−diffusion system functions analogously to a grounded shield in electronics that prevents external noise from reaching the electronic instrument. As the volume of the moat is much larger than the volume of the well, the moat acts as a constant boundary condition for the well that the moat encloses, effectively isolating the well from any chemicals that could otherwise diffuse through the PDMS to the well from outside the moat. Importantly, once the system has been sealed, the moat and well are isolated from the bulk exchange of BZ solution via advection, although they remain diffusively coupled by the permeation of chemicals through the PDMS. The concentrations of the BZ reagents used here are the same as those used previously.[17] Additionally, to obtain better statistics, we manufacture devices with four wells and moats to perform four independent experiments simultaneously, as seen in Figure 2A.

Since chemical reaction rates are highly temperature-dependent, we use a homemade closed-loop temperature control system to maintain a temperature of 22 ± 0.1 °C throughout the duration of the experiment.[27]

We use a homemade programmable illumination microscope (PIM) that has two functions: (1) visualize the BZ oscillation to measure the period and (2) control the BZ oscillation by projecting light that interacts with the photosensitive catalyst, $Ru(bpy)_3^{2+}$.[1,28] The PIM consists of two discrete arms, one for each of the two functions.

The BZ visualization arm is a 4× magnification microscope that uses transmitted light that passes through the BZ sample and is imaged on a charge-coupled device (CCD) camera. The illumination source is a 510 nm light-emitting diode (LED). The absorption spectra differ between the oxidized and reduced states of BZ, with the reduced state having a higher absorption of 510 nm light. This wavelength was chosen to give the maximum contrast between the reduced and oxidized states of BZ. A series of time lapse images of the oscillating BZ solution in the wells reveal the oxidation state as maxima in the intensity of the transmitted light, shown in Figure 2B. We locate these maxima in the intensity as a function of time using a peak detection algorithm, from which we determine the oscillation period of the BZ solution.

The control arm utilizes a computer projector as a programmable light source in the epi-illumination, or reflection, configuration of the microscope. Blue light from the computer projector of wavelength 425−500 nm is shone onto the BZ sample. Light of this wavelength and sufficient intensity suppresses the BZ oscillation and sets the BZ solution in a steady state that has chemical concentrations similar to those in the reduced state of the oscillating reaction. Thus, we

https://dx.doi.org/10.1021/acs.jpcb.0c08422
J. Phys. Chem. B XXXX, XXX, XXX−XXX

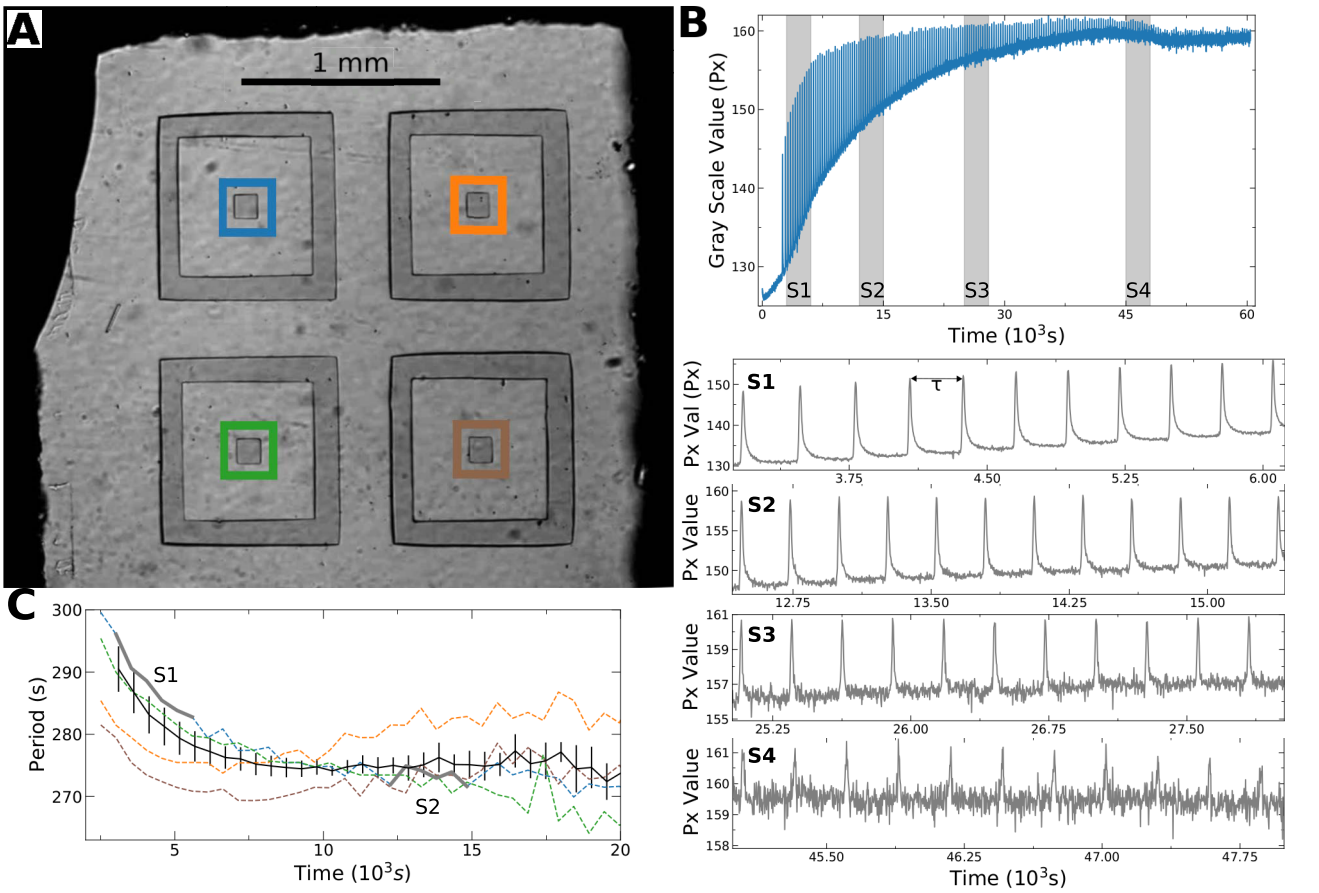

Figure 2. BZ oscillations in PMDS wells with a 2 μm thick layer of PDMS. (A) Photograph of the BZ-filled wells surrounded by BZ-filled moats. Each well is isolated from the system by the moats. Each of the wells has been color-coded to correspond with the measured periods as a function of time that are plotted in (C). A video of a representative experiment is included in the Supporting Information. (B) Intensity trace as a function of time over the course of an experiment. The blue curve shows the gray scale value of a well as a function of time, over long time scales. The gray vertical bars correspond to the times shown in the images below. The graphs below show the intensity trace as a function of time for a duration of 3 ks. The start times are 3.1 ks (S1), 12.4 ks (S2), 25 ks (S3), and 45 ks (S4). Using a peak detection algorithm, we are able to find peaks in the gray scale value, which correspond to the oxidized BZ state. The time interval between these intensity peaks is the oscillation period. (C) Measured periods vs time for four wells. The color of each dotted line corresponds to measurements obtained from the like-colored wells in (A). The solid gray lines marked S1 and S2 correspond to the periods of the intensity trace intervals in (B). The black line corresponds to the average period of the wells, with the error bars showing the standard error for each period. A total of 70 oscillations were observed during this time interval.

use the control arm of the PIM to apply actinic light to the moat with a spatial accuracy of 10 μm.

For a typical experiment, we record time lapse series of images for 20 000 s. Images are recorded during the time intervals when no light is being projected onto the moat. This view is shown in Figure 2A. To extract a period from the raw data, we average the intensities of each pixel in each well for every frame in the video to create a plot of the transmitted intensity through the wells as a function of time, as shown in Figure 2B. The maximum transmitted intensity occurs during oxidation of the ruthenium, resulting in a series of bright flashes. A video of a representative experiment is included in the Supporting Information. We find the period by measuring the time duration between spikes. The sealed BZ well is a closed system and oscillates about 200 times before the reactants are consumed and oscillations cease. However, as the signal-to-noise ratio decreases over time, we stop the experiment after about 70 oscillations. Each data set contains four discrete wells, allowing us to define an average and standard deviation for the data set for every oxidation spike as a function of time (Figure 2C).

Prior to running an experiment, we seal the BZ in the microfluidic chip using a homemade clamp. Sealing the BZ solution in a manner that allows photographing the BZ reaction in a microscope while projecting actinic light, maintaining a constant temperature, preventing leaks, and suppressing generation of CO_2 bubbles is tricky. For example, to transmit forces from the clamp to the PDMS to effectively seal the wells, it is important to have only a small area of glass in contact with the PDMS. The 3 mm × 3 mm gray region visible in Figure 2A is the PDMS underneath the "sealing window", and the outer black region is the BZ solution. For details, see the Supporting Information, Movie S7 and Figure S1 in Litschel et al.[17] Additionally, before we run the experiments, we leave the sealed sample in a dark space for 20 min. This increases the photosensitivity of our BZ. Furthermore, the moats often oscillate if we skip this waiting period. We postulate that this behavior relates to the concentration of bromomalonic acid and dibromomalonic acid in the chemical mix. Bromomalonic acid is a chemical consumed in one of the pathways of the photoinhibition processes. However, the initial BZ reagents do not contain bromomalonic acid, which is generated during the BZ reaction.

https://dx.doi.org/10.1021/acs.jpcb.0c08422
J. Phys. Chem. B XXXX, XXX, XXX−XXX

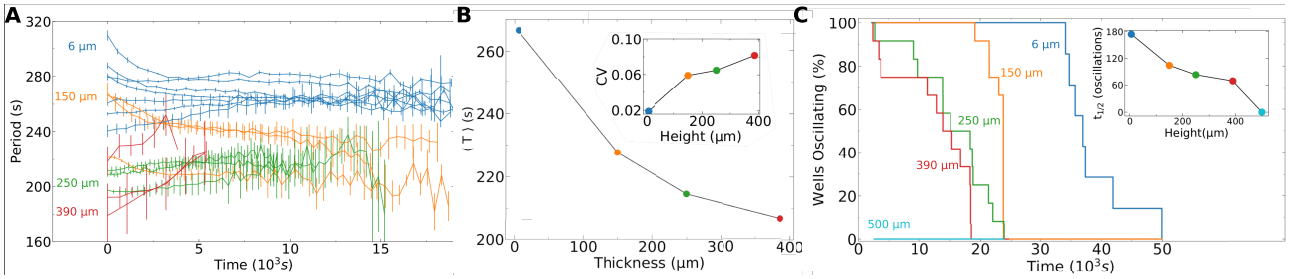

Figure 3. Effects of PDMS height on BZ oscillations. (A) Oscillation period vs time for wells with different thicknesses (L) of PDMS. The thicknesses were 6, 150, 250, and 390 μm, corresponding to blue, orange, green, and red curves, respectively. Each line represents the average of four wells measured at the same time. The error bars show the standard error for the four wells. (B) Average period (T) as a function of PDMS thickness. The inset plot shows the coefficient of variation (CV) of period as a function of PDMS thickness. The coefficient of variation is the standard deviation of a set of values divided by the mean of those values. (C) Percentage of wells remaining oscillating as a function of time. The 100% mark corresponds to the total population of 12 oscillating wells at the start of the experiment. Wells of height 500 μm and above never oscillate, so they are reported with 0% oscillating. The inset figure shows the half-life of the samples in units of number of oscillations as a function of the PDMS thickness.

Thus, it is necessary to wait long enough to generate enough bromomalonic acid for the photoinhibition process to function.[29−31]

To study the effects of PDMS on the behavior of the BZ oscillator, we vary the thickness of the PDMS layer underneath the well while using the same feature geometry. For these experiments, we use thicknesses of 6, 150, 250, 390, and 500 μm. Additionally, we examined the role of boundary conditions by eliminating the moats used to establish a constant boundary condition. All other features and dimensions of the microfluidic device remained the same, with the dimensions of the well being w = 120 μm and d = 30 μm with a volume of 0.43 nl. We did not vary the dimensions of the wells for these experiments. An example of the raw data, similar to the experiment described in Figure 2, is included in the Supporting Information (Movie S1).

We exploit the BZ's light sensitivity to gain active control over the chemistry within the well. As the light perturbs the BZ off the limit cycle, we can apply the light in two ways to modify the phase and the frequency of the BZ. To modify the phase of the BZ oscillations, we apply a continuous short duration pulse of light with a high intensity. As the light sensitivity depends on the chemical concentrations within the BZ and as the concentrations change periodically with time, perturbations at different points in the BZ cycle will generate different responses. In our experiments, we track the phase of the BZ and perturb with an intense light at nine equally spaced phases in the BZ cycle. Additionally, we vary the exposure time from 3 to 15 s, allowing us to further control the phase.

We change the period of the well by continually shining a low-intensity light on the sample, which is enough to increase the oscillation period without completely suppressing the oscillations. We first find the critical intensity, which suppresses all oscillations in the well, I_c. We then vary the intensity of the light across a range of values to find the relationship between the intensity of light and the frequency of oscillation.

Since the BZ chemistry is sensitive to light, we homogenize the intensity of light projected by the PIM to 10% across the sample for all levels of projected intensity. If we do not homogenize the light, the computer projector is much brighter in the center of the sample and falls off by a factor of 2 at the edges of the sample. To homogenize the light, we instruct the computer projector to project a grid of squares onto the sample plane of the microscope. Our projector allows control of the intensity value of each projected pixel. Initially, each of the projected squares is set to the same intensity value. We place a two-dimensional (2D) light detector, consisting of the CCD array of a video camera without a lens, in the sample plane. A software feedback loop is used to tune the intensity values of each projected square until every square measured by the CCD reaches the identical target intensity. We then interpolate between the intensity values of the projected squares to create a continuous map of the intensity values of the projector that are necessary to form a uniform intensity image in the sample plane. We did this for a series of target intensities and measured that the light intensity varied less than 10% across the sample for all intensities.

RESULTS AND DISCUSSION

Measuring BZ Oscillation Period as a Function of PDMS Thickness. Devices were constructed in which the thickness of PDMS beneath a well was increased while holding all other geometrical features constant. The period of oscillation was measured as a function of time, shown in Figure 3A. Several trends emerged, as shown in Figure 3B,C. First, we examined the average period, T, shown in Figure 3B. The oscillation period decreased with increasing thickness of the PDMS layer (Figure 3B). The wells with the thinnest bottom layer of 6 μm had the longest period with $\langle T \rangle$ = 268 s. Wells with a bottom layer of 150 μm had an appreciably shorter oscillation period of $\langle T \rangle$ = 227 s. However, as the PDMS thickness increased further, the oscillation period trended toward a constant value. Additionally, as the PDMS became thicker, the variation in the oscillation period increased. The coefficient of variation (CV), defined as the standard deviation of the period of the four wells divided by their mean period is plotted as a function of thickness in the inset in Figure 3B. The coefficient of variation increased with PDMS thickness. Finally, we measured the fraction of wells that remain oscillating as a function of time (Figure 3C). The half-life of a BZ oscillator, $t_{1/2}$, defined as the time at which half of the oscillators have ceased oscillating is plotted in the inset of Figure 3C. With increasing PDMS thickness, the half-life decreases and above a critical thickness of PDMS of about 500 μm, the wells never oscillated and the half-life was zero (inset of Figure 3C).

https://dx.doi.org/10.1021/acs.jpcb.0c08422
J. Phys. Chem. B XXXX, XXX, XXX−XXX

Modeling BZ Oscillation Period as a Function of PDMS Thickness. We construct a simple reaction−diffusion model consisting of three points, as shown in Figure 4A. The first point describes the BZ in a well, the second point the PDMS separating the well and the moat, and the third point the moat. To model the chemistry, we use the Vanag−Epstein model, which reduces the BZ chemistry to a system of four differential equations, each modeling a different chemical concentration: bromous acid, bromide, oxidized catalyst, and bromine.[32] Using this chemical model, we assume that only bromine can permeate into PDMS, that bromine can react with the PDMS and be consumed, and that Fick's law describes the diffusive coupling. For this work, the reaction rate is set by the concentration of reactants within the PDMS and is assumed to be constant. Details of the model are provided in the Supporting Information.

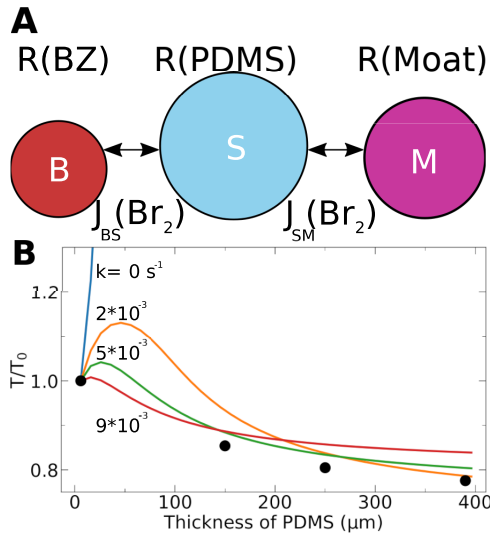

Figure 4. Simulation of BZ oscillations with bromine loss in PDMS. (A) Schematic of the theory with three zones of reaction (R). BZ (red, "B") is simulated using the four-variable Vanag−Epstein model. A loss reaction occurs in the PDMS (blue, "S"). The moat (purple, "M") is simulated using the four-variable Vanag−Epstein model with light. Diffusive fluxes (J) couple the bromine between the reaction zones. (B) Fractional simulated period change as a function of PDMS volume. Different lines represent different reaction rate constants within the PDMS. The black dots show experimental data for the fractional period as a function of PDMS thickness, normalized by the period with a PDMS thickness of 6 μm.

When the reaction rate between the PDMS and bromine is zero, the calculated period of the BZ oscillation increases as a function of thickness. The explanation is that the PDMS acts as a reservoir of bromine. When the concentration of bromine is low in the well containing BZ, then bromine flows from the PDMS reservoir into the BZ well, which has the effect of increasing the bromine concentration in the BZ solution. As bromine converts to inhibitor, an increase in bromine concentration increases the oscillation period.

In contrast, when the reaction rate between bromine and PDMS is large, the period of the BZ oscillation decreases as a function of the PDMS thickness. A large reaction constant between bromine and PDMS means the bromine in the PDMS is rapidly consumed. Then, the concentration of bromine in the PDMS is always lower than the bromine concentration in the BZ solution resulting in a flux of bromine out of the BZ solution. Removing bromine from the oscillator decreases the concentration of inhibitor, thereby decreasing the oscillation period.

In Figure 4B, we find that the best agreement between theory and experiment is when the model allows bromine to both permeate into and react with the PDMS. The fitted loss rate is $k = 5 \times 10^{-3}$ s^{-1}. From this reaction rate and the effective diffusion constant of bromine in PDMS, D, we can define a reaction−diffusion length scale, λ, using the equation

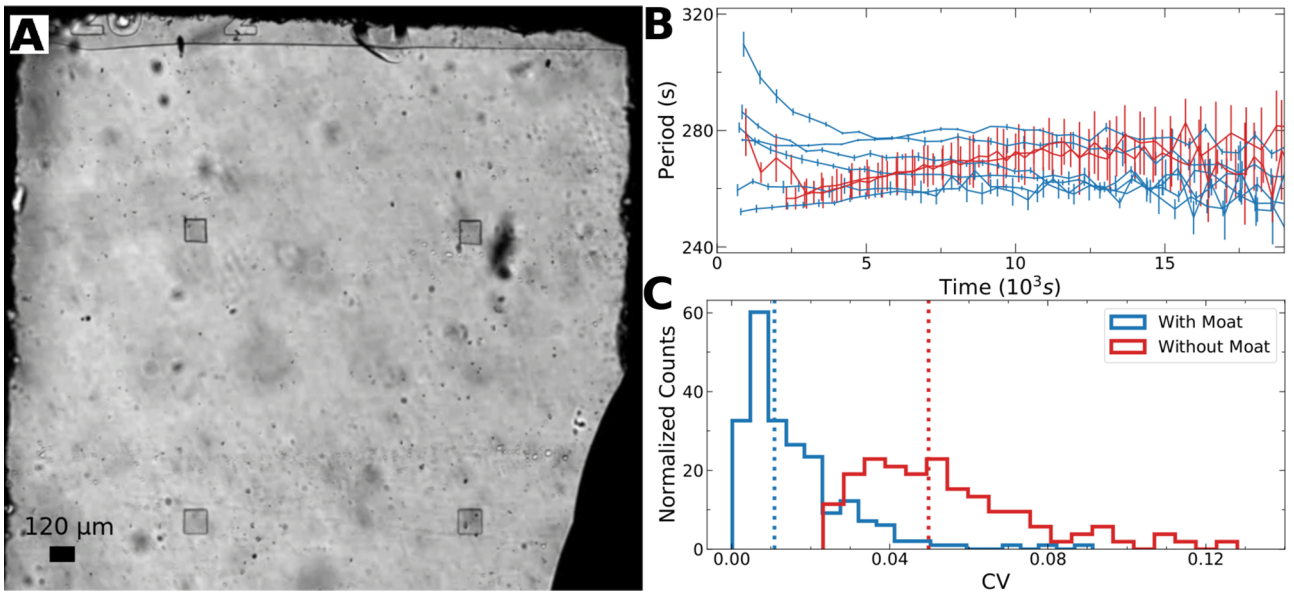

Figure 5. BZ oscillations without moats. (A) Photograph of BZ wells with no moat. (B) Oscillation period as a function of time for wells with (blue) and without (red) moats. The PDMS thickness for both samples is 6 μm. (C) Histogram of the coefficient of variation of the period for wells with and without moats. The dotted lines show the median coefficient of variation for wells with moats (blue) and without moats (red). The histogram is normalized, such that the area under each histogram is one.

https://dx.doi.org/10.1021/acs.jpcb.0c08422
J. Phys. Chem. B XXXX, XXX, XXX−XXX

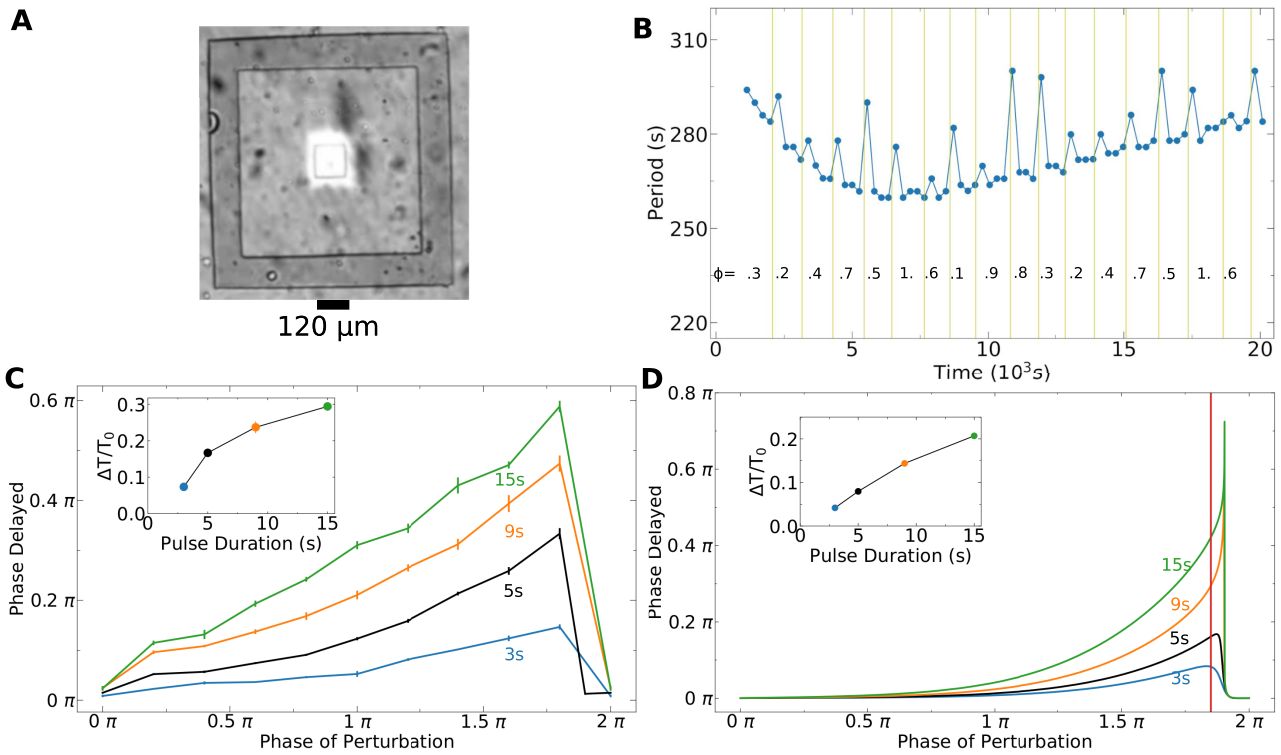

Figure 6. Phase response curve of BZ oscillations to light. (A) Photograph of a well containing BZ illuminated with light to perturb the phase. (B) Measured BZ periods (points) as a function of time. The moments at which light perturbation was applied are marked with vertical yellow lines and labeled with the phase at which the perturbation occurred. The perturbed period is the subsequent blue dot following the perturbation. (C) Experimental phase response curve. Each colored curve corresponds to a different exposure duration, labeled with the same color. The inset plot shows the maximum phase delay in units of the fraction of the oscillation period as a function of the perturbation duration. (D) Simulated phase response curve. Each colored curve corresponds to a different exposure time, labeled with the same color. The inset plot shows the phase delay as a function of the perturbation duration at the phase corresponding to the phase in the experiment that gave the maximum of the PRC (red vertical line).

$$\lambda = \sqrt{\frac{D}{k}}$$

Using D = 375 μm^2 s^{-1} (see the Supporting Information), we obtain a reaction−diffusion length scale of about 275 μm for bromine in PDMS. This result is consistent with the observation that BZ oscillations cease in PDMS wells with walls thicker than 500 μm.

Effect of the Moat on the BZ Oscillation Period. We compare BZ oscillations in devices with and without moats in our thinnest devices, which have 6 μm thick layers of PDMS under the well (Figure 5). The mean oscillation period of the wells without moats closely matches the mean period of wells with moats. However, the median coefficient of variation is nearly 5 times larger for wells without moats compared to that for wells with moats, CV = 0.050 vs 0.011, respectively. We conclude that establishing constant boundary conditions in the vicinity of the wells significantly reduces experimental noise by isolating one well from another and from the environment.

Phase Response Curve (PRC). The phase response curve (PRC) is the shift in period induced by a unit perturbation as a function of the phase of the oscillator.[33] The ruthenium BZ system is light-sensitive, and we use pulses of light projected by the PIM onto the well to perturb the phase, as seen in Figure 6A.[17,24,28] To determine the phase of the well before perturbation, we let the well oscillate unperturbed for two full periods and assume that the phase increases linearly with time. For these experiments, we use a microfluidic device with a 2 μm thick layer of PDMS beneath the wells and we surround each well with a moat. To avoid systematic bias, we randomly choose one of nine phases linearly spanning the interval $[0, 2\pi]$, repeating once until we sampled all nine phases (Figure 6B). We determine the PRC by measuring the time interval between the observed and expected BZ oscillations. If the observed oscillation is delayed and occurs later than expected for the unperturbed oscillator, we say that light inhibited the oscillation. We fixed the intensity of the PIM, measured in the sample plane, at 3 mW cm^{-2}, which was the highest intensity that we could achieve for the PIM while using our light homogenization protocol. We illuminated the entire well and generated phase response curves using exposure times of 3, 5, 9, and 15 s, shown in Figure 6C. For a given exposure time, we observe an increase in the phase delay as a function of phase, with a maximum phase delay at a phase of 90% of the well's period. The phase response curve increases in amplitude as a function of the exposure time, with the maximum phase delay increasing less than linearly as a function of exposure time, as shown in the inset of Figure 6C. The maximal elongation of the period of oscillation was observed to be 30% of the unperturbed period.

We use the Vanag−Epstein model to compare the measured light-induced PRC with theory, as explained in detail in the Supporting Information.[32] We simulate the same phase perturbations used in experiment and also vary the exposure times of the perturbations. Qualitatively, the theory generates phase response curves that are similar to experiment; both

https://dx.doi.org/10.1021/acs.jpcb.0c08422
J. Phys. Chem. B XXXX, XXX, XXX−XXX

show a small phase delay for low values of phase, with an increasing phase response as a function of the phase (Figure 6C,D). The theoretical PRC has a maximum delay that occurs immediately before the BZ reaction produces an oxidation spike, in contrast to experiment in which the peak in the PRC occurs at 90% of the phase. With increasing exposure duration, each of the calculated phase response curves also shows an increased phase delay. However, the slope of the experimental curve is linear, while the theory curve increases with a higher power of the phase. There is good correspondence between theory and experiment in the magnitude of the phase delay at a phase of 90% of a period, which corresponds with the peak delay in the experimental system.

Frequency Response Curve. To alter the frequency of the BZ, we again use light to perturb the system, shown in Figure 7A. This time, instead of using pulses of light, we use constant exposure to uniform intensity light. As previously, we measure the period of the unperturbed oscillator before perturbing the oscillator by applying light. In the absence of any applied light, we measure three periods of BZ oscillations and then apply light of a given intensity for three periods. This allows us to account for the slow variations in the period of a BZ oscillator as a function of time, as shown in Figure 2C. Next, we establish the critical level of light necessary to completely suppress oscillations, I_c. Then, we apply light with intensities below I_c. The lowest light intensity is 11% of I_c, and we increase intensity in increments of 11% of I_c. To avoid systematic bias, we randomize the order in which we apply the various intensities. As the intensity of light applied to the well increases, the increase in period begins to diverge. Below 66% of the critical intensity, the change in period is reproducible with a very small amount of variation. However, above 66% of the critical intensity, the change in period becomes much more varied, and there is an increase in the number of nonoscillating wells.

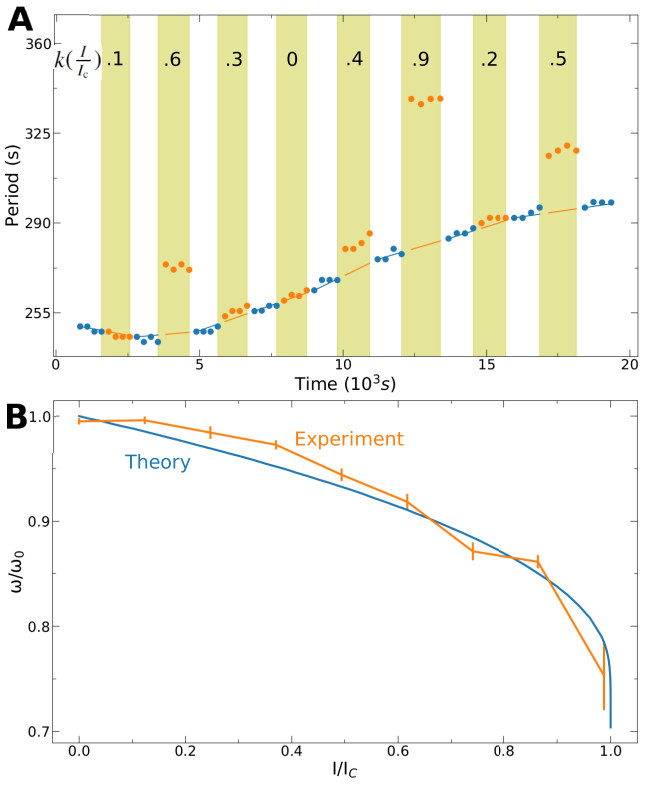

Figure 7. Frequency response curve of BZ oscillations to light. (A) Measured oscillation period as a function of time. The yellow (white) background indicates light applied (not applied) to the BZ in wells. The annotations in the yellow zones indicate the normalized intensity with the value 1.0 just sufficient to suppress oscillations. Orange (blue) points represent data with light applied (not applied). The blue lines represent the best linear fits for the periods with no light applied. The orange lines represent a linear interpolation from the data with no light. (B) Frequency as a function of applied intensity. Orange represents the normalized experimental oscillation frequency as a function of the normalized intensity of light. The frequency is normalized by the frequency with no light applied, and the intensity is normalized by the critical intensity of light. Error bars indicate the standard error. The blue line represents the calculated normalized frequency as a function of the normalized photogeneration rate. The frequency is normalized by the frequency of BZ with no light applied, and the photogeneration rate is normalized to the photogeneration rate which suppresses oscillation in the simulated BZ.

We once more use simulation to explain the behavior of the BZ oscillators exposed to light. We calculate the oscillation period of the BZ as a function of the photogeneration rate of BZ, $k(I)$, explained in detail in the Supporting Information. To compare theory and experiment, we normalize the period with respect to the period of an unperturbed well and the photogeneration rate to the critical photogeneration rate, which suppresses BZ oscillation. Normalizing the experimental data in the same manner produces a good agreement between experiment and theory, as shown in Figure 7B.

CONCLUSIONS

We studied the behavior of the BZ oscillating reaction when compartmentalized into sub-nanoliter volumes, referred to as wells, in devices fabricated from the elastomer PDMS. The lifetime of a BZ oscillator decreased approximately linearly with the thickness of the PDMS beneath the wells. The lifetime went to zero, e.g., no oscillations were ever observed in a population of 12 independent oscillators, when the PDMS beneath the bottom of the wells was thicker than 500 μm. In order for the oscillations to be long-lived, stable, and reproducible, it was important to reduce the amount of PDMS beneath the wells to be less than 10 μm and to establish controlled boundary conditions by surrounding the wells with a moat filled with BZ held in a steady state through the application of light. Furthermore, through the application of light, we were able to change the period and phase of the oscillators by up to 30%. Numerical modeling of the oscillation period as a function of the amount of PDMS surrounding the BZ compartments suggests that the inhibitory species bromine both permeates into and reacts with the PDMS. Our numerical model produced an estimate of the reaction−diffusion length of bromine in a PDMS of 275 μm, consistent with the observation that wells in PDMS devices thicker than 500 μm did not oscillate. Furthermore, we find a near-quantitative agreement between computational models and experiments on the effect of light on the BZ oscillations. The characterization of individual wells and moats, and the measurement and calculation of the phase and frequency response curves for light presented here establish the engineering foundations for the rationale design of larger, complex, addressable, and controllable reaction−diffusion networks of BZ oscillators in PDMS.

https://dx.doi.org/10.1021/acs.jpcb.0c08422
J. Phys. Chem. B XXXX, XXX, XXX−XXX

■ ASSOCIATED CONTENT

Supporting Information

The Supporting Information is available free of charge at https://pubs.acs.org/doi/10.1021/acs.jpcb.0c08422.

Description of the thermal controls implemented in the experiments; additionally, the supplement details the parameters of the theoretical model we use for the BZ, as well as the reaction−diffusion and light perturbation models used in the paper (PDF)

A movie showing four oscillating BZ wells surrounded by moats; movie has been sped up by a factor of 160 and the wells sit on top of a 2 μm thick layer of PDMS; oscillations in the moats are suppressed by the application of light from a computer projector, however, the light from the computer projector is only shone onto the sample when the camera is not recording images, therefore one never sees the moat illuminated in the video (AVI)

■ AUTHOR INFORMATION

Corresponding Author

Seth Fraden − *Department of Physics, Brandeis University, Waltham, Massachusetts 02453, United States*; Phone: 781-736-2888; Email: fraden@brandeis.edu

Authors

James Sheehy − *Department of Physics, Brandeis University, Waltham, Massachusetts 02453, United States*; orcid.org/0000-0001-8368-1160

Ian Hunter − *Department of Physics, Brandeis University, Waltham, Massachusetts 02453, United States*; orcid.org/0000-0002-7730-6628

Maria Eleni Moustaka − *Department of Physics, Brandeis University, Waltham, Massachusetts 02453, United States*

S. Ali Aghvami − *Department of Physics, Brandeis University, Waltham, Massachusetts 02453, United States*

Youssef Fahmy − *Department of Physics, Brandeis University, Waltham, Massachusetts 02453, United States*

Complete contact information is available at: https://pubs.acs.org/10.1021/acs.jpcb.0c08422

Notes

The authors declare no competing financial interest.

■ ACKNOWLEDGMENTS

We thank Amanda Chisholm for her work on the graphical interface used for the work. S.F. and J.S. devised the experiments. S.A.A., M.E.M., and J.S. designed the microfluidic setups and fabricated devices using a technique devised by M.E.M. Y.F., S.A.A., and I.H. designed the temperature control used for the experiment. I.H. and J.S. implemented light control for the microscope. J.S. performed the experiments and simulation and analyzed both. S.F. and J.S. developed the figures. We would like to acknowledge funding from NSF DMREF-1534890 and the U.S. Army Research Laboratory and the U.S. Army Research Office under Contract/Grant No. W911NF-16-1-0094. We would also like to acknowledge funding of the microfluidics facility at Brandeis, which was funded through NSF MRSEC DMR-2011486.

■ REFERENCES

(1) Delgado, J.; Li, N.; Leda, M.; González-Ochoa, H. O.; Fraden, S.; Epstein, I. R. Coupled oscillations in a 1D emulsion of Belousov-Zhabotinsky droplets. *Soft Matter* **2011**, *7*, 3155−3167.

(2) Torbensen, K.; Rossi, F.; Ristori, S.; Abou-Hassan, A. Chemical communication and dynamics of droplet emulsions in networks of Belousov-Zhabotinsky micro-oscillators produced by microfluidics. *Lab Chip* **2017**, *17*, 1179−1189.

(3) Rossi, F.; Zenati, A.; Ristori, S.; Noël, J.; Cabuil, V.; Kanoufi, F.; Abou-Hassan, A. Activatory Coupling Among Oscillating Droplets Produced in Microfluidic Based Devices. *Int. J. Unconv. Comput.* **2015**, *11*, 23−36.

(4) Fullarton, C.; Draper, T. C.; Phillips, N.; de Lacy Costello, B. P.; Adamatzky, A. Belousov-Zhabotinsky reaction in liquid marbles. *J. Phys.: Mater.* **2019**, *2*, No. 015005.

(5) Gizynski, K.; Gorecki, J. Chemical memory with states coded in light controlled oscillations of interacting Belousov-Zhabotinsky droplets. *Phys. Chem. Chem. Phys.* **2017**, *19*, 6519−6531.

(6) Guzowski, J.; Gizynski, K.; Gorecki, J.; Garstecki, P. Microfluidic platform for reproducible self-assembly of chemically communicating droplet networks with predesigned number and type of the communicating compartments. *Lab Chip* **2016**, *16*, 764−772.

(7) Carballido-Landeira, J.; Vanag, V. K.; Epstein, I. R. Patterns in the Belousov-Zhabotinsky reaction in water-in-oil microemulsion induced by a temperature gradient. *Phys. Chem. Chem. Phys.* **2010**, *12*, 3656−3665.

(8) Toiya, M.; González-Ochoa, H. O.; Vanag, V. K.; Fraden, S.; Epstein, I. R. Synchronization of chemical micro-oscillators. *J. Phys. Chem. Lett.* **2010**, *1*, 1241−1246.

(9) Proskurkin, I. S.; Vanag, V. K. Dynamics of a 1D array of inhibitory coupled chemical oscillators in microdroplets with global negative feedback. *Phys. Chem. Chem. Phys.* **2018**, *20*, 16126−16137.

(10) Thutupalli, S.; Herminghaus, S. Tuning active emulsion dynamics via surfactants and topology. *Eur. Phys. J. E* **2013**, *36*, 91.

(11) Tompkins, N.; Li, N.; Girabawe, C.; Heymann, M.; Ermentrout, G. B.; Epstein, I. R.; Fraden, S. Testing Turing's theory of morphogenesis in chemical cells. *Proc. Natl. Acad. Sci. U.S.A.* **2014**, *111*, 4397−4402.

(12) Tompkins, N.; Cambria, M. C.; Wang, A. L.; Heymann, M.; Fraden, S. Creation and perturbation of planar networks of chemical oscillators. Chaos: An Interdisciplinary. *J. Nonlinear Sci.* **2015**, *25*, No. 064611.

(13) Li, Y.-N.; Chen, L.; Cai, Z.-S.; Zhao, X.-z. Experimental study of chaos synchronization in the Belousov-Zhabotinsky chemical system. *Chaos, Solitons Fractals* **2004**, *22*, 767−771.

(14) Li, N.; Tompkins, N.; Gonzalez-Ochoa, H.; Fraden, S. Tunable diffusive lateral inhibition in chemical cells. *Eur. Phys. J. E* **2015**, *38*, 1−12.

(15) Wilson, D.; Faramarzi, S.; Moehlis, J.; Tinsley, M. R.; Showalter, K. Synchronization of heterogeneous oscillator populations in response to weak and strong coupling. Chaos: An Interdisciplinary. *J. Nonlinear Sci.* **2018**, *28*, No. 123114.

(16) Norton, M. M.; Tompkins, N.; Blanc, B.; Cambria, M. C.; Held, J.; Fraden, S. Dynamics of Reaction-Diffusion Oscillators in Star and other Networks with Cyclic Symmetries Exhibiting Multiple Clusters. *Phys. Rev. Lett.* **2019**, *123*, No. 148301.

(17) Litschel, T.; Norton, M. M.; Tserunyan, V.; Fraden, S. Engineering reaction-diffusion networks with properties of neural tissue. *Lab Chip* **2018**, *18*, 714−722.

(18) Brandrup, J.; Immergut, E. H.; Grulke, E. A.; Abe, A.; Bloch, D. R. *Polymer Handbook*; Wiley: New York, 1999; Vol. *89*.

(19) Ginn, B. T.; Steinbock, B.; Kahveci, M.; Steinbock, O. Microfluidic Systems for the Belousov- Zhabotinsky Reaction. *J. Phys. Chem. A* **2004**, *108*, 1325−1332.

(20) Buskohl, P. R.; Vaia, R. A. Belousov-Zhabotinsky autonomic hydrogel composites: Regulating waves via asymmetry. *Sci. Adv.* **2016**, *2*, No. e1600813.

(21) Li, N.; Delgado, J.; González-Ochoa, H. O.; Epstein, I. R.; Fraden, S. Combined excitatory and inhibitory coupling in a 1-D array

of Belousov-Zhabotinsky droplets. *Phys. Chem. Chem. Phys.* **2014**, *16*, 10965−10978.
(22) King, P. H.; Corsi, J. C.; Pan, B.-H.; Morgan, H.; de Planque, M. R.; Zauner, K.-P. Towards molecular computing: Co-development of microfluidic devices and chemical reaction media. *Biosystems* **2012**, *109*, 18−23.
(23) Cabrera, J. N.; Ruiz, M. M.; Fascio, M.; D'Accorso, N.; Mincheva, R.; Dubois, P.; Lizarraga, L.; Negri, R. M. Increased surface roughness in polydimethylsiloxane films by physical and chemical methods. *Polymers* **2017**, *9*, 331.
(24) Wang, A.; Gold, J.; Tompkins, N.; Heymann, M.; Harrington, K.; Fraden, S. Configurable NOR gate arrays from Belousov-Zhabotinsky micro-droplets. *Eur. Phys. J.: Spec. Top.* **2016**, *225*, 211−227.
(25) Friend, J.; Yeo, L. Fabrication of microfluidic devices using polydimethylsiloxane. *Biomicrofluidics* **2010**, *4*, No. 026502.
(26) Ren, L.; Fan, B.; Gao, Q.; Zhao, Y.; Luo, H.; Xia, Y.; Lu, X.; Epstein, I. R. Experimental, numerical, and mechanistic analysis of the nonmonotonic relationship between oscillatory frequency and photointensity for the photosensitive Belousov-Zhabotinsky oscillator. Chaos: An Interdisciplinary. *J. Nonlinear Sci.* **2015**, *25*, No. 064607.
(27) Adamatzky, A.; Fullarton, C.; Phillips, N.; De Lacy Costello, B.; Draper, T. C. Thermal switch of oscillation frequency in Belousov-Zhabotinsky liquid marbles. *R. Soc. Open Sci.* **2019**, *6*, No. 190078.
(28) Tompkins, N.; Fraden, S. An inexpensive programmable illumination microscope with active feedback. *Am. J. Phys.* **2016**, *84*, 150−158.
(29) Yamaguchi, T.; Shimamoto, Y.; Amemiya, T.; Yoshimoto, M.; Ohmori, T.; Nakaiwa, M.; Akiya, T.; Sato, M.; Matsumura-Inoue, T. Bromomalonic acid as a source of photochemically produced Br- ion in the Ru (bpy) 32+-catalyzed Belousov-Zhabotinsky reaction. *Chem. Phys. Lett.* **1996**, *259*, 219−224.
(30) Kádár, S.; Amemiya, T.; Showalter, K. Reaction Mechanism for Light Sensitivity of the Ru (bpy) 32+-Catalyzed Belousov-Zhabotinsky Reaction. *J. Phys. Chem. A* **1997**, *101*, 8200−8206.
(31) Vanag, V. K.; Zhabotinsky, A. M.; Epstein, I. R. Role of Dibromomalonic Acid in the Photosensitivity of the Ru (bpy) 32+-Catalyzed Belousov- Zhabotinsky Reaction. *J. Phys. Chem. A* **2000**, *104*, 8207−8215.
(32) Vanag, V. K.; Epstein, I. R. A model for jumping and bubble waves in the Belousov-Zhabotinsky-aerosol OT system. *J. Chem. Phys.* **2009**, *131*, No. 104512.
(33) Izhikevich, E. M. *Dynamical Systems in Neuroscience*; MIT Press, 2007; Chapter 10.

https://dx.doi.org/10.1021/acs.jpcb.0c08422
J. Phys. Chem. B XXXX, XXX, XXX−XXX